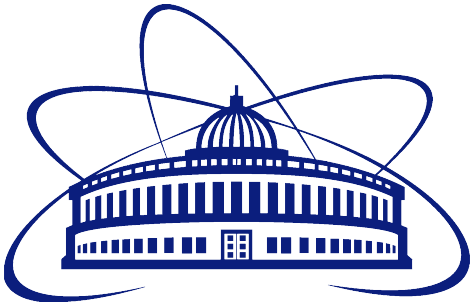

JOINT INSTITUTE FOR NUCLEAR RESEARCH

Veksler and Baldin laboratory of High Energy Physics

Final report of the START programme

Collider Mode (Reduced Magnetic Field)

Particle identification determination of spectra using information about the energy losses (dE/dx) in the TPC and the Time-of-flight from the TOF detector.

Supervisor

Dr. Viktar Kireyeu

Student

San Juan López

Alejandro

Universidad Autónoma Metropolitana

Summer Session 2024. July 06th - August 27th, Dubna 2024

Abstract

The process by which particles are identified in high-energy experiments requires a thorough process to study the interaction of particles in the different sensitive elements of the detector. In particular the MPD uses the TPC and the TOF to obtain the energy loss and square mass distributions (both dependent on the particle moment), which are described by functions such as that of Bethe-Bloch, whose parameters must be obtained in a detailed manner for each particle species, by means of an adjustment which allows the regions where each particle species is found to be delimited and thus eliminates contamination by other particles. This report describes all these steps to obtain a correct identification of particles generated in collisions of BiBi with the MPD under reduced magnetic field conditions in collider mode, This analysis is important because at the date of this report there is no documentation of the detector response under these conditions.

keywords: Energy Loss, Fit Function, Monte Carlo tracks, reconstructed tracks, Bethe-Bloch equation, Eficiency, Parameters, Gaussian Function

Resumen

El proceso mediante el cual se hace la identificación de partículas en los experimentos de altas energías, requiere de un proceso minucioso para estudiar la interacción de las partículas en los diferentes elementos sensibles del detector. En particular el MPD utiliza la TPC y el TOF para obtener las distribuciones de pérdida de energía y masa cuadrada (ambas dependientes del momento de la partícula), las cuales son descritas por funciones como la de Bethe-Bloch, cuyos parémetros deben ser obtenidos de manera minuciosa para cada especie de partícula, a através de un ajuste que permita delimitar las regiones donde se encuentra cada especie de partícula y con ello eliminar la contaminación por parte de otras partículas. En este reporte se describen todos estos pasos para obtener una correcta identificación de las partículas generadas en colisiones de BiBi con el MPD bajo condiciones de campo magnético reducido en el modo colisionador, este análisis es importante ya que a la fecha de este reporte aun no hay documentación de la respuesta del detector en estas condiciones.

Contents

1 Introduction **2**
- 1 Main problem . . . 2
  - 1.1 Project goals . . . 2
- 2 Background . . . 3
  - 2.1 Nuclotron-based Ion Collider fAcility (NICA) . . . 3
  - 2.2 Physics behind NICA . . . 3
  - 2.3 Multi-Purpose Detector (MPD) . . . 4

2 Theoretical framework **6**
- 1 The energy losses (dE/dx) . . . 6
- 2 Collider Mode . . . 8
- 3 Reduce Magnetic Field . . . 8

3 Metodology **9**
- 1 Momentum-dependent square mass and energy loss histograms . . . 9
- 2 Fitting functions for each charged particle . . . 11
  - 2.1 Adjustment by Gaussian function . . . 11
  - 2.2 Adjustment by Bethe-Bloch function . . . 12
- 3 The correct distribution of dE/dx . . . 15
- 4 Efficiency of the detected particles . . . 17

4 Results **19**
- 1 Adjustment functions for each particle species . . . 19
- 2 Energy loss distributions . . . 25
- 3 Efficiency histograms . . . 28

5 Conclusions **31**

6 Acknowledgments **32**

Chapter 1

Introduction

The scientific progress in physics requires a theoretical framework and experimental measurements, in the latter case for fundamental physics of elementary particles, large laboratories are needed, based on huge accelerators and gigantic detectors, The aim is to disintegrate matter into its most fundamental elements and to have a data collection large enough to have an adequate statistic to determine physical observables with sufficient accuracy. This is the importance of the START programme, which aims to train students in solving scientific tasks under the supervision of experts in the area for a period of 8 weeks.

1 Main problem

1.1 Project goals

The specific objective is based on the analysis of data available in "Request 28. UrQMD BiBi@9.2", for collider mode with reduced magnetic field. The analysis of these data and results are of great importance as they form part of detector performance under different initial conditions as low magnetic field. The analysis of the data was carried out with my colleague Physicist. Juan Carlos Marquez, through complementary activities, which were:

- **Task 1.** [1]Primary vertex determination and Particle Track reconstruction, optimization of cuts in η, pT, number of hits on TPC.
- **Task 2.** Particle identification determination of spectra using information about the energy losses (dE/dx) in the TPC and the Time-of-flight from the TOF detector.

As mentioned in the title of this report, the activity I developed was task 2 using the wagon and class system implemented for MPDRoot simulation software, which consisted of the following objectives:

1. Get the momentum dependence of the average energy loss and the mass squared resolution for charged particles.
2. Get Particle identification efficiency as a function of momentum with TPC.
3. Comparison of results with default magnetic field.

[1]If you want to know more about the work developed by my colleague you can consult the page of GitHub [10], as well as the written report `https://start.jinr.ru/index.php?session_id=5`

2 Background

2.1 Nuclotron-based Ion Collider fAcility (NICA)

In contemporary theoretical understanding, matter can exist in several states: hadronic matter, quark and gluon plasma and a transition process called "mixed phase". High-density baryonic matter is virtually unexplored. For its experimental study, it is necessary to create baryonic matter in the extreme conditions of collisions of heavy ions at high energies. To this end, the NICA project was launched in 2008. The basic design configuration will allow for acceleration and collision of heavy ions, up to gold ions, in the optimum energy range from the minimum in the zone of extracted beams to the maximum achievable $\sqrt{s_{NN}} = 11$ GeV (for Au^{+79}, in the nucleon-nucleon center of mass system) in the collider, with an average luminosity of $L = 10^{27}$ $cm^{-2}s^{-1}$. This will allow the study of nuclear matter in a state of maximum baryonic density, inaccessible to research in other laboratories around the world.

The NICA accelerator complex consists of two chains of light ($A/Z = 1 \div 3$) and heavy ion injection ($A/Z = 1 \div 6$), the booster synchrotron and nuclotron synchrotron, two superconducting collider storage rings and beam transport channels between these elements. The light ion injection chain creates, accelerates and transports ions to the Nuclotron; the heavy ion injection chain also transports them to the Booster from where they are transported to the Nuclotron after acceleration. The Nuclotron provides broad-spectrum ion beams (from protons to gold) to applied research facilities, the BM@N experiment and the Collider, using slow and fast beam extraction systems and corresponding particle transfer channels. The main facility of the complex, which provides experiments at MPD and SPD facilities, is the Collider. Consists of two storage rings placed one on top of the other with two interaction points (IP). Beam collisions are carried out at a zero angle.

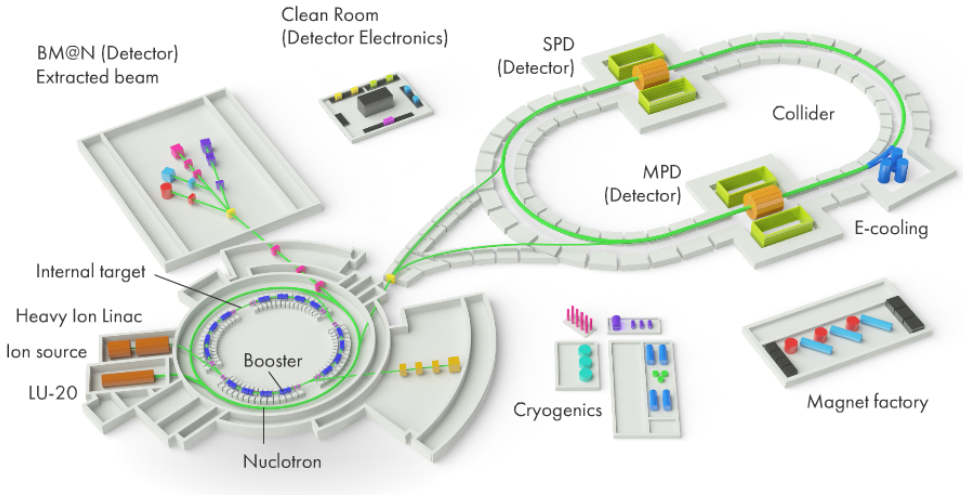

Figure 1.1: *Arrangement of the main accelerators and experimental facilities in the NICA complex. [19]*

2.2 Physics behind NICA

As mentioned, the NICA project is focused on studying the properties of nuclear matter in the region of maximum baryonic density. Such matter existed only in the early stages of

the evolution of our universe and in the interiors of neutron stars. The QCD (Quantum Chromodynamics) calculations predict both the phase transition of unconfinement and the restoration of chiral symmetry occurring at sufficiently high energy densities, and there is strong experimental evidence that the unconfined phase of nuclear matter (Quark and Gluon Plasma - QGP) can be created in ultra-high energy nuclear collisions.

The energy range in which NICA works (3 to 11 GeV) is wide enough to cover both collisions where the plasma phase is well developed and collisions where matter remains purely hadronic. In addition to determining the existence and location of the transition region, it is of fundamental interest to establish the character of the associated phase transformation, namely whether it remains a smooth transition or has become one of first order as predicted by various models. In the latter case, the phase diagram of the strongly interacting matter must contain a critical point and its experimental identification constitutes a focal point for this field of research.

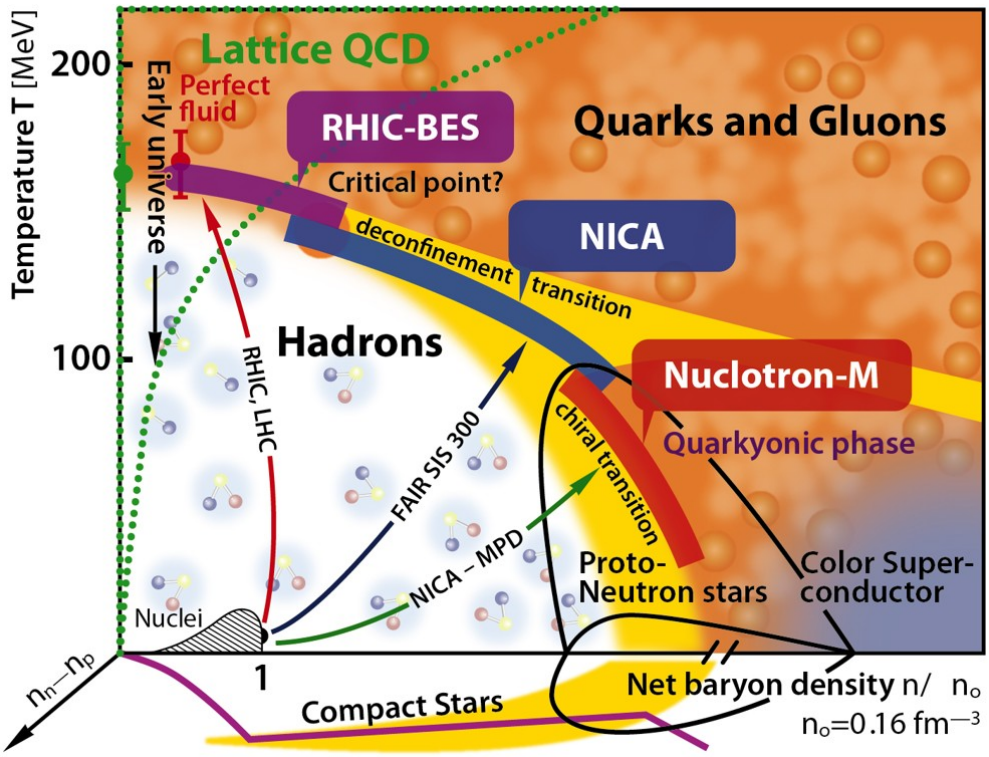

Figure 1.2: *Diagram of the QCD [19].*

2.3 Multi-Purpose Detector (MPD)

The multi-purpose detector (MPD) is one of two experiments dedicated to heavy ion complex collisions (NICA). Its main scientific objective is to search for new phenomena in the baryon-rich region of the quantum chromodynamics phase diagram (QCD), at an energy range of 3 $< \sqrt{S_{NN}} <$ 11 GeV for ion species ranging from protons to Au^{79+}.

The first stage of MPD assembly is scheduled for 2025, which consists of the superconducting solenoid, the Time Projection Chamber (TPC), the Time of Flight system (TOF), the Electromagnetic Calorimeter (ECal), the Forward Hadron Calorimeter (FHCal) and the

Fast Forward Detector (FFD).

In addition, it is expected that detectors like the miniBeBe will be placed between the beam tube and the TPC, close to the beam, designed to assist in the activation and timing of the start of the TOF.

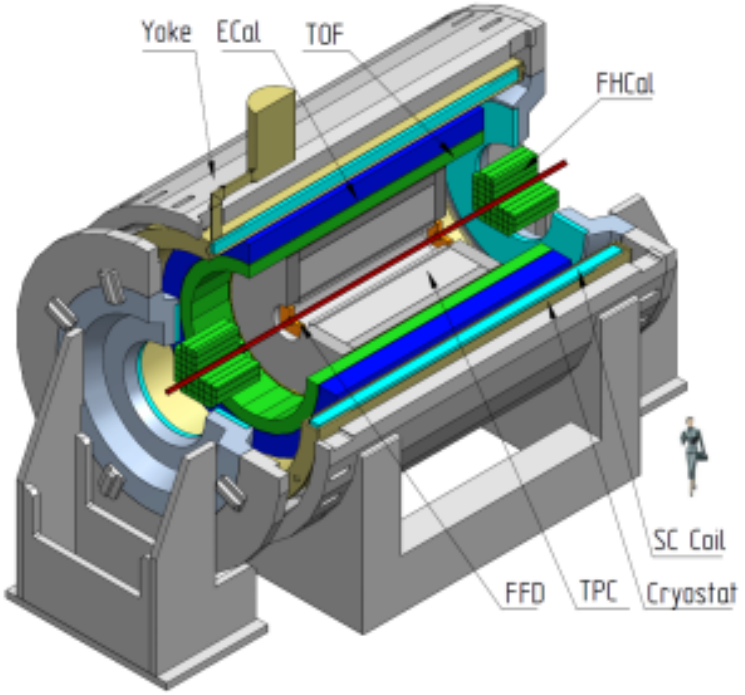

Figure 1.3: *Basic configuration of the MPD Central Detector.[16]*

Chapter 2

Theoretical framework

1 The energy losses (dE/dx)

Loss of energy by ionization is the process by which a charged particle loses energy as it passes through a medium, such as a detector. This loss of energy is crucial for particle identification in experimental particle physics. By measuring the loss of ionizing energy (dE/dx), along with the moment of the particle, you can identify the type of particle and determine its kinetic energy.

The theoretical expression that predicts loss of ionizing energy (the mean rate of energy loss) is the *Bethe - Bloch equation* (2.1), which describes how the loss of energy increases proportionally with β^{-2} as the particle velocity decreases. This equation also takes into account the density of the medium through which the particle is moving.

$$\langle -\frac{dE}{dx} \rangle = K z^2 \frac{Z}{A} \frac{1}{\beta^2} \left[\frac{1}{2} ln \frac{2 m_e c^2 \beta^2 \gamma^2 W_{max}}{I^2} - \beta^2 - \frac{\delta(\beta\gamma)}{2} \right]. \tag{2.1}$$

The energy loss is not the same for each particle, as it depends on the charge, mass and velocity of the particle, as well as the material through which it is moving, the description of these and other variables on which the equation (2.1) depends are found in table 2.1. Slower particles are more ionizing than faster particles, and energy loss reaches a minimum for a specific velocity range, known as the minimum ionization particle regime (see figure 2.1).

For MPD, the loss of ionization energy will change according to the detector material through which the particles travel. For example, the TPC detector will measure the ionization of charged particles in a gas, while the TOF detector will measure the flight time of particles through a solid material. Both detectors will provide valuable information on particle energy loss, and it is for this reason that they are used in combination to identify and characterize charged particles in MPD experiments.

Symb.	Definition	Value or (usual) units
E	energy	MeV
x	mass per unit area	g cm^2
K	coefficient for dE/dx	0.307075 MeV mol^{-1} cm^2
z	charge number of incident particle	
Z	atomic number of absorber	
A	atomic mass of absorber	g mol^{-1}
$m_e c^2$	electron mass x c^2	0.5109989461(31) MeV
I	mean excitation energy	eV
$\delta(\beta\gamma)$	density effect correction to ionization energy loss	
W_{max}	Maximum possible energy transfer to an electron in a single collision	MeV

Table 2.1: *Variables of Bethe equation. The kinematic variables β and γ have their usual relativistic meanings.*

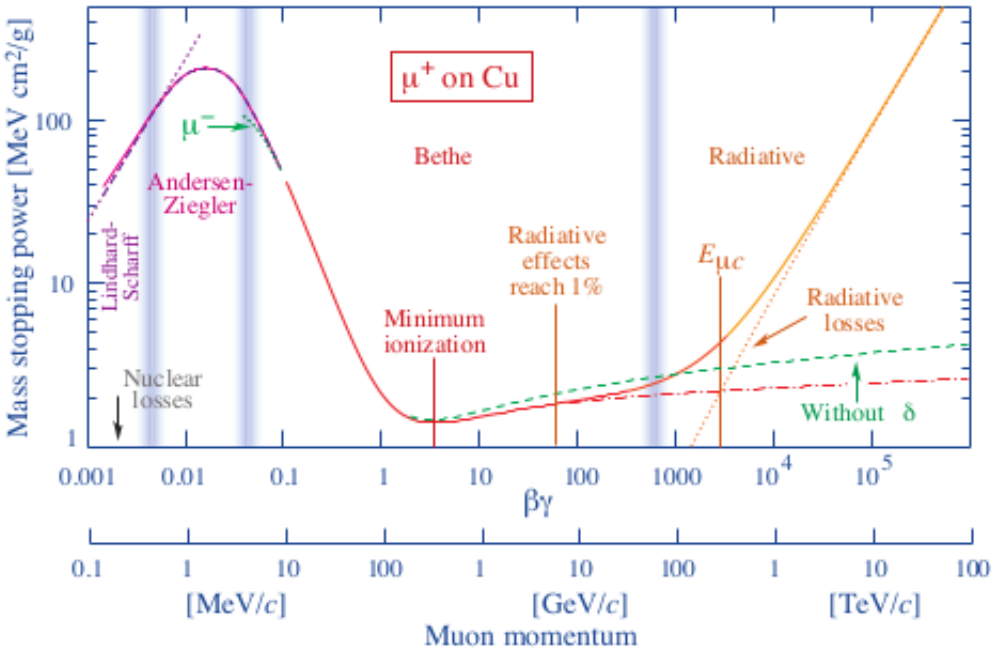

Figure 2.1: *Energy loss of muons in copper. The y-axis is given in units of MeV cm^2 /g so that one can multiply by the density of any material and compute the energy loss in MeV/cm. The energy loss depends on the relativistic quantity $\beta\gamma$ which can be converted to momentum [11].*

As you can see in the figure 2.1, we will have different regions marked by vertical lines. This implies that the energy loss will have a different behavior at low and high energies. This behavior in the dE/dx function will be reflected as corrections to the Bethe-Bloch equation; that is, terms will be added or removed to adjust the function. Some of these corrections are: shell correction, Barkas correction and Bloch correction. In addition, there will be other proposed functions that can describe the behavior of energy loss in these regions. One of them is the Landau-Vavilov-Bichsel function.

According to the energy region studied by the MPD ($3 < \sqrt{S_{NN}} < 11$ GeV) indicates that the distribution of energy loss expected to follow particles corresponds to the region of minimum ionization.

2 Collider Mode

The NICA project assumes the use of 3 modes of the accelerator complex operation and, correspondingly, 3 different operating modes of the Collider.

- Mode 1. The accumulation of heavy ions in the Collider, their acceleration and formation of a bunched ion beams, and performing experiments on colliding beams.
- Mode 2. The mode of asymmetric collider: accumulation of various types of ions, preparation of colliding beams like in Mode 1 and performing experiments on colliding beams of heavy and light ions.
- Mode 3. The mode of polarized beams: accumulation of polarized protons and/or deuterons acceleration, the same procedure of beams formation and performing experiments on spin physics with colliding beams of polarized particles.

3 Reduce Magnetic Field

The importance of studying what happens to the collision mode when the magnetic field is reduced lies in the fact that the way we reconstruct particles is based on the trajectory formed by the transverse momentum when interacting with the magnetic field. In other words, thanks to the magnetic field, we can correctly reconstruct particles through their transverse momentum.

However, there are particles with low transverse momentum that, even with the full magnetic field (Bz = 5 kG), are not significantly affected. These particles are trapped rotating within the Time Projection Chamber (TPC), preventing them from reaching the detector limits and, therefore, they cannot reach other detectors.

This situation makes it difficult to accurately reconstruct this type of particle with low transverse momentum. Since we want to reconstruct and record all particles, we seek to reduce the magnetic field to evaluate if we can thus improve the reconstruction of these particles.

It should be noted that this study is only analyzing the case of a reduced magnetic field in the TPC. However, studies will also be conducted where the magnetic field will be increased by a factor of 2, with the aim of exploring all possible scenarios.

Chapter 3

Metodology

The methodology for the development of the following activities is based on the report [21], carried out during the INTEREST programme, but with some changes according to what was learned during the START programme. Therefore, for certain steps in the procedure, only such a report will be referred to.

1 Momentum-dependent square mass and energy loss histograms

The first step to start with the particle identification process was to obtain the histograms of energy loss and square mass as a function of momentum, for this a new system of wagons was written, where the main class containing important tasks is named "EnerClass1.cxx", the set of all classes used can be found on the GitHub[1] page [10].

As mentioned in the report [21], tasks in a class are classified into three functions: UserInit, ProcessEvent and Finish. For our class we defined the histograms of the particles to be analyzed (proton, kaon, deuterium, pion, tritium, He^3 and He^4) within the UserInit function, as shown in the code 3.1.

Listing 3.1: Example of some defined histograms

```
void EnerClass1::UserInit(){
.
.
//histogram for dE/dx
  h__dedxHe3 = new TH2F("h_dedx_He^{3}", "dEdx vs P for the helium 3; p*q GeV/
      c; dE/dx arb.units",300, -1.5, 1.5, 600, 0.0, 60);
        fOutputList->Add(h__dedxHe3);
//histogram for m^2
  h__m2He3 = new TH2F("h__m2He3", "m^{2} vs P for the Helium3; p*q GeV/c; m
      ^{2} GeV^{2}/c^{4}", 200, -4.0, 4.0, 200, -1.0, 2.0);
        fOutputList->Add(h__m2He3);
.
.
}
```

Once the histograms were defined, the code for the analysis of the events available in "Request 28. UrQMD BiBi@9.2 (table 3.1)" for reduced magnetic field was written.

[1]The file path is: AlejandroSJuan/EnerClass/simplept/EnerClass1.cxx

Parameters	Information
Event generator	UrQMD
Collision	Bi + Bi
Energy	9.2 GeV
Number of events analysed	10,500,000
Magnetic field	2 kG

Table 3.1: *Parameters of the data analysed*

For this process, within the ProcessEvent function, the branches required for analysis were established, which were: GetGlobalTracks, fTPCKalmanTrack, fMCTrack and fTOF-Matching. After, within a loop for belonging to the reconstructed tracks the restriction of values for the analyzed data is realized, this restriction is introduced in the code as cuts for the observable ones of the table 3.2, the specific value of these cuts were obtained and provided by my co-worker phys. Juan Carlos Marquez Ramirez[2].

Observable	Value
Number of hits	> 27
Pseudorapidity	$-1.5 < \eta < 1.5$
Global DCA	> 1 cm
Primary vertex position	$-50 < Vtx < 50$
Transverse momentum	pT > 0.15 GeV/c

Table 3.2: *Range of values in observable ones to obtain a cleaner distribution.*

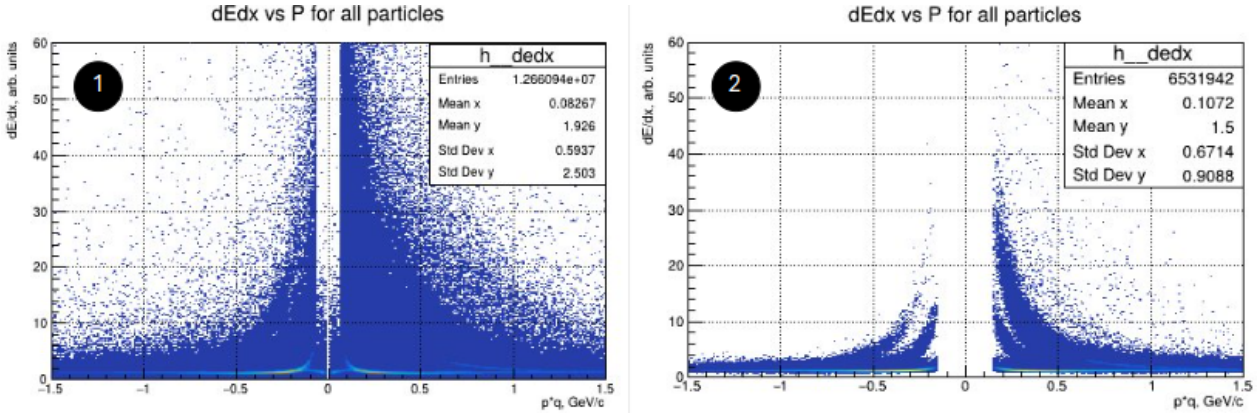

Figure 3.1: *Energy loss histogram for all particle species.1-Shows the histogram without implementation of the cuts, 2- Shows the histogram with implemented cuts.*

Once the cuts were made (as can be seen in the figure 3.1), each histogram was filled for each particle using the information of the moment (p), square mass (m^2) and energy loss (de/dx), which can only be taken from the reconstructed tracks "KalmanTracks", since it contains the information of the collision simulation taking into account the detectors. The classification of particles was carried out by conditional if and the PDG code corresponding to each particle, as you can see in the code 3.2.

[2]To know how these cuts were obtained, you can consult the report [12]

Listing 3.2: Example of classification of the particles and their respective histograms

```
void EnerClass1::ProcessEvent(MpdAnalysisEvent &event){
    .
    .
        if (pdg == 1000020030)
        {
                //He3
                h__dedxHe3->Fill(p, dedx);
                h__m2He3 -> Fill(p, mpdtrack -> GetTofMass2());

         }else if (pdg == 1000020040)
         {
                //He4
                h__dedxHe4->Fill(p, dedx);
                h__m2He4 -> Fill(p, mpdtrack -> GetTofMass2());
         }else if (pdg == 1000010030)
         {
                //Tritio(t)
                h__dedxt->Fill(p, dedx);
                h__m2t -> Fill(p, mpdtrack -> GetTofMass2());
         }else if (pdg == 1000010020)
         {
                //Deuterion (d)
                h__dedxd->Fill(p, dedx);
                h__m2d -> Fill(p, mpdtrack -> GetTofMass2());
         }
    .
    .
}
```

Something to clarify is that all the histograms defined in "EnerClass1.cxx", must also be called in "EnerClass1.h"

2 Fitting functions for each charged particle

2.1 Adjustment by Gaussian function

Obtained the histograms of energy loss and square mass, both depending on the moment, we proceeded to adjust the region of maximum particle density by means of an adjustment function, which had the objective of delimiting this region.

One important thing to clarify is that the histograms used to carry out the following procedure were obtained without the restriction of the cuts of the table 3.2, because they were not yet defined, it is important to clarify this because it may be one of the reasons why the results are not as expected, which will be discussed later.

For all histograms a procedure similar to the one explained (in more detail) in the report [21] was followed, This procedure is based on making cuts over the projection of the "de/dx" and "m^2" axes of each histogram, in order to obtain parameters that will help us define the best possible function.

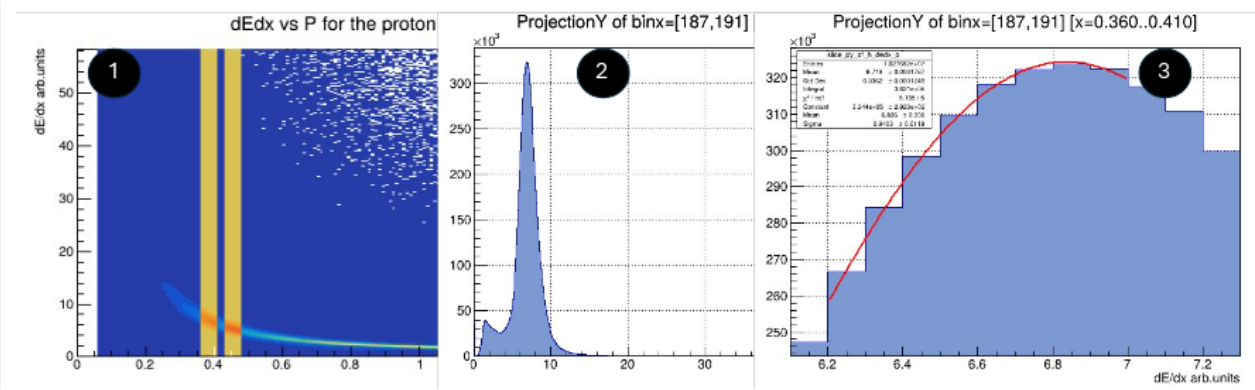

Figure 3.2: *Example of the process for obtaining the value of the parameters for the proton adjustment function. 1-Shows the selection region (yellow bar), 2-Projection of the selected region on the dE/dx axis, 3-Adjustment of the distribution by a Gaussian function (red line).*

As shown in figure 3.2, the cuts were made with the help of the graphical environment of MpdRoot, the selection of the cuts was established by the number of bins, this value could vary, but for most cases a value equal to five was chosen. Once the region of the cut was defined, an adjustment was made by a gaussian function, because it is the one that worked best, something to consider for this adjustment was the value of "Chi-square per degree of freedom", since it must be the closest to one, and other important values of this adjustment were the mean value and sigma, as well as their respective errors.

2.2 Adjustment by Bethe-Bloch function

Obtained the values for the cuts, which give us information about the maximum peak of the function, we proceeded to make a macro 3.3 that allowed us to get the correct adjustment function according to the data obtained.

Listing 3.3: Macro "FitPronocut.C" to get the adjustment function for protons using the values obtained "data1" and "data2"

```
//Bethe-Bloch equation for protons
Double_t parPr(Double_t *x, Double_t *p)
{
   Double_t x1, x2, x3,ans;

   x1  = p[0] / TMath::Power(x[0] / TMath::Sqrt(x[0] * x[0] + 0.88), p[3]);
   x2  = p[1] - TMath::Power(x[0] / TMath::Sqrt(x[0] * x[0] + 0.88), p[3]);
   x3  = TMath::Log(p[2] + TMath::Power(1.0 / (x[0] / 0.9383), p[4]));
   ans = x1 * (x2 - x3);

   return ans;
}
 void FitPronocut(){

    //Histogram dE/dx
     TFile *file1 = new TFile("/home/alejandro/Documentos/EnerClass/Fit-
         functions/taskEnerAll.root");
     TH2F *h_dedx_p = (TH2F*)file1->Get("h_dedx_p");

 //--mean values of Gaussian functions and their errors
    const int nBins=18;
    Stat_t data1[nBins
       ]={24.9622,17.9635,13.1672,9.88914,7.81359,6.31973,5.25655,4.47178
    ,3.88242,3.43243,3.07454,2.78969,2.56354,2.37552,2.22018,2.09064
    ,1.98205,1.89001};

    const int nError=18;
    Stat_t data2[nError
       ]={0.0258993,0.0148647,0.0167922,0.00605115,0.0039364,0.00293919
    ,0.00411013,0.00169941,0.0015333,0.000743479,0.000772767,0.000642989
    ,0.00035937,0.000349082,0.000448932,0.000292752,0.000237986,0.000234231};

     TH1F *fa1 = new TH1F("dEdx_proton", "dE/dx-parameterization-for-the-
         proton;-p*q-GeV/c;-dE/dx-arb.units", 18, 0.13, 1.09);

     for(int i=0; i<nBins; i++){
     fa1->SetBinContent(i+1,data1[i]);
       for (int j=0; j<nError; j++){
         fa1->SetBinError(j+1,data2[j]);
       }
     }

     TF1 *fitparPr = new TF1("fitparPr",parPr,0.13,1.09,5);

     h_dedx_p->Draw("same");
     fa1->Draw("same");
     fa1->Fit("fitparPr");
 }
```

As shown in the macro 3.3 the proposed fit function is given by equation (3.1), which is a simplification of the Bethe-Bloch equation, and which is implemented in the class MpdPid.cxx [14] from which it was obtained,

$$\langle \frac{dE}{dx} \rangle = \frac{P_0}{\beta^{P_3}} \left[P_1 - \beta^{P_3} - ln\{P_2 + \left(\frac{1}{\beta\gamma} \right)^{P_4} \} \right], \qquad \beta = \frac{p}{\sqrt{p^2 + M^2}}, \tag{3.1}$$

where $P_{N=0,..,4}$ are the parameter of the function and p the moment.

because this function is dependent on the mass of particles (in units of $\frac{GeV}{c^2}$) it will be different for each particle, so we have different macros[3].

The operation of the macro 3.3 (and for other particles) is as follows:

1. The Bethe-Bloch equation is defined for each particle

2. Within the function "void"" you can call the energy loss histogram of the particle to be analyzed, from the file generated (taskEnerAll.root) by the file "RunAnalyses. C" and implement the mean values and their respective errors, which were obtained previously when adjusting the Gaussian function

3. By a loop **for** the values are assigned to a function "fa1" to define the points where there is more density of particles, then these points are adjusted by another function (fitparPr) dependent on the equation of Bethe-Bloch

4. Run the macro to get the parameters of the equation (code 3.4)

Also, as shown in the code 3.3, the values of "nBins" and "nError" are 18[4], which represents the necessary degrees of freedom to obtain a good value for the 5 parameters on which the equation (3.1) depends.

Listing 3.4: Parameters of the adjustment function for the proton obtained after executing the macro "FitPronocut.C"

```
Minimizer is Minuit2 / Migrad
Chi2                      =      6049.25
NDf                       =           13
Edm                       =       42.752
NCalls                    =         1632
p0                        =     -1.24869   +/-   0.00342623
p1                        =      0.39063   +/-   0.00431698
p2                        =      1.51189   +/-   0.00322369
p3                        =     0.822324   +/-   0.00103526
p4                        =      2.74567   +/-   0.00427964
```

[3]The macro for each particle is located on the GitHub page [10] within the path: AlejandroSJuan/EnerClass/Fit functions.

[4]For the other particle adjustments, values between 12 and 18 were taken, but always greater than 5.

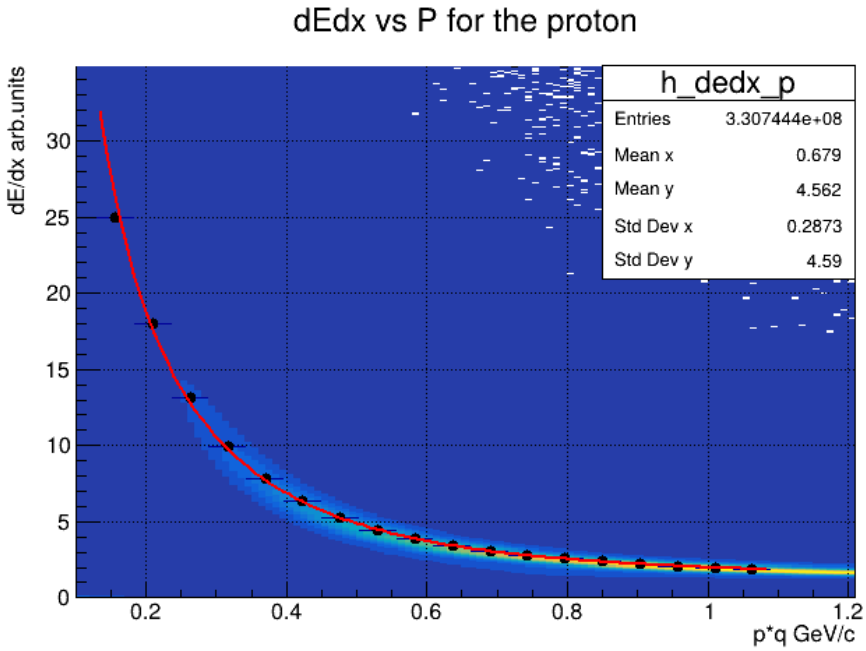

Figure 3.3: *Adjustment function obtained for the proton energy loss histogram.*

3 The correct distribution of dE/dx

Once the correct parameters for the Bethe-Bloch equation of each particle are obtained and it is verified that this function fits well our distribution, the next step will be to delimit the region where there is more concentration of particles, so to do this, we need to add and subtract to the mean value (dE/dx), the value of multiples of the previously obtained value of σ.

The main reason for delimiting the region is that we need to eliminate all those particles that are different from the species we are identifying, because the amount of particles per species in the reconstruction of tracks unlike the monte carlo (MC) tracks must be smaller, this requires us to know specifically the percentage of particles identified when passing through the detectors after the collision.

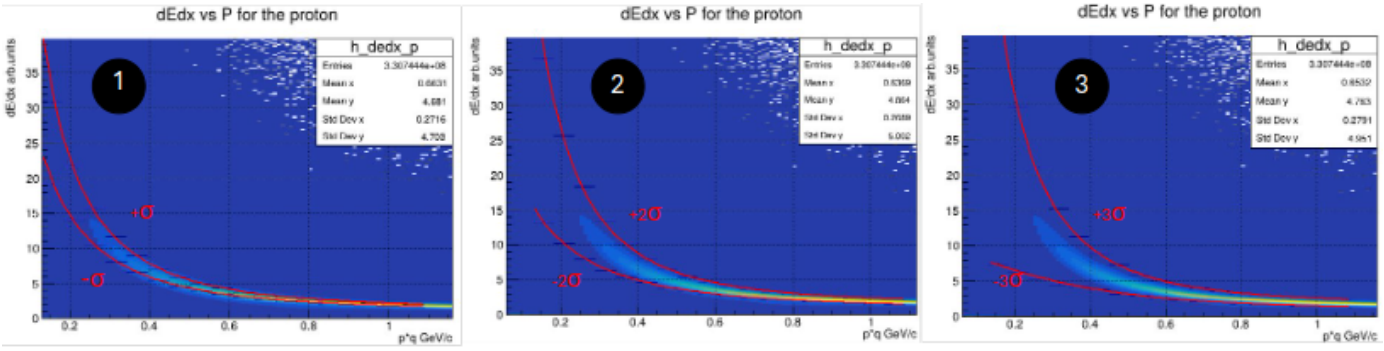

Figure 3.4: *Regions bounded by different sigma values. 1-Shows the region restricted by mean*$\pm 1\sigma$*, 2-Shows the region restricted by mean*$\pm 2\sigma$*, 3-Shows the region restricted by mean*$\pm 3\sigma$*.*

As can be seen in figure 3.4, choosing a multiple of different sigma delimits a greater or lesser region, because it is known that about 68% of the value obtained from a normal distribution lies within a range of one σ (standard deviation), for the work carried out on this project the option that was chosen was to add $\pm 1\sigma$. Once the region was delimited, a similar process was carried out to obtain the parameters of the functions $+\sigma$ and $-\sigma$, the macros that perform this function can be found on the page of GitHub [10] in the path: AlejandroSJuan/EnerClass/Sigma functions, these macros will show us on the screen the value of the parameters after they are executed.

	proton		kaon		pion	
Parameter	$+1\sigma$	-1σ	$+1\sigma$	-1σ	$+1\sigma$	-1σ
P0	-2.58072	-3.70863	-0.817989	-0.564779	-0.327131	-0.182489
P1	1.16569	1.70197	-0.332111	-1.11641	-2.32774	-3.16187
P2	1.97189	2.64031	0.452453	0.799115	-0.340479	0.899613
P3	0.782313	0.434546	2.51922	0.808589	3.94556	3.10849
P4	2.20629	2.0007	0.356776	3.07986	-0.371293	-0.836771

Table 3.3: *Parameters of the Bethe-Bloch equation for the limit functions "dEdx+1σ" and "dEdx-1σ".*

Once the parameters for the Bethe-Bloch equations of the sigmas were obtained, they were declared within the class "EnerClass1.cxx", then set as limits of the value of "dE/dx", as shown in code 3.5,

Listing 3.5: Example of how to introduce limits for the value of "dE/dx"

```
//_____Bethe Bloch functions for each
    particle_____________________________________________________

//Proton_sigma_____________________________________________
  double dedxp1=((-2.58072) / TMath::Power(p / TMath::Sqrt(p * p + 0.88),
      0.782313))*((1.16569 - TMath::Power(p / TMath::Sqrt(p * p + 0.88),
      0.782313))-(TMath::Log(1.97189 + TMath::Power(1.0 / (p / 0.9383),
      2.20629))));//proton+1sigma

  double dedxp2=((-3.70863) / TMath::Power(p / TMath::Sqrt(p * p + 0.88),
      0.434546))*((1.70197 - TMath::Power(p / TMath::Sqrt(p * p + 0.88),
      0.434546))-(TMath::Log(2.64031 + TMath::Power(1.0 / (p / 0.9383), 2.0007)
      )));//proton-1sigma
.
.
//Limits in dE/dx of the
    proton_____________________________________________________
        if(dedx >= dedxp2 && dedx <= dedxp1 ){

          PtProreco1->Fill(pt_reco);
          if(pdg == 2212){ //we use the pdg code to clean up more signal and
              get the real particles
                h__dedxpcut->Fill(p,dedx);
                PtProreco2->Fill(pt_reco);
           }
        }
```

By doing the above we get a cleaner signal, as can be seen in figure 3.5. This process was repeated only for three particles: protons, kaons and pions.

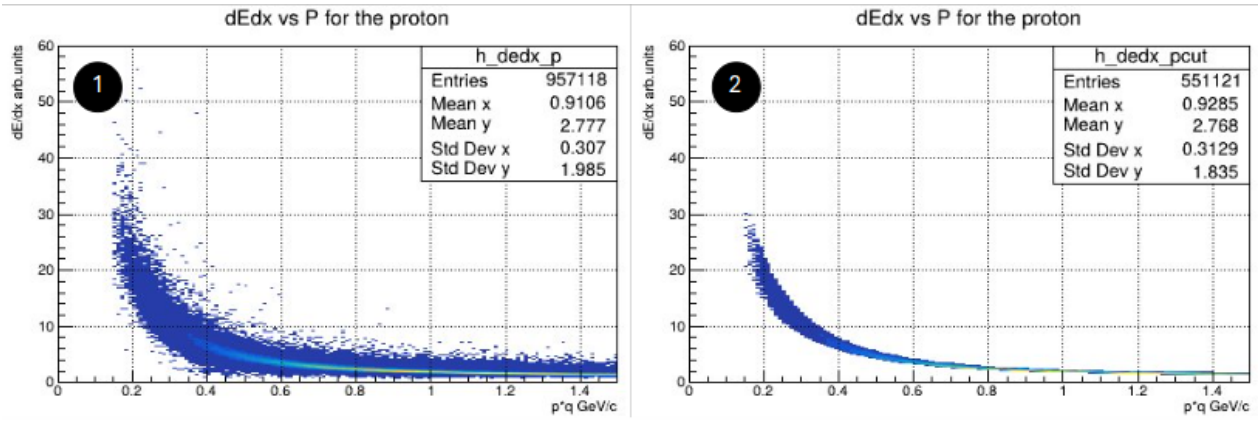

Figure 3.5: *Distribution of energy loss for the proton. 1-Show distribution only using PDG selection, 2-Show distribution using limits for the value of dE/dx and classification by PDG.*

4 Efficiency of the detected particles

Once a cleaner signal is obtained, the next important thing to know is the difference in the number of particles detected after data reconstruction (KalmanTracks) and those obtained from the ideal collision simulation (Monte Carlo Tracks). For this, transverse moment histograms (pT) were obtained for three specific particles: protons, kaones and pions, in three cases: pT histogram for monte carlo tracks, pT histograms for reconstructed tracks only with restriction on dE/dx boundaries and pT histograms again for reconstructed tracks, but with restriction on dE/dx boundaries and PDG code classification of particles (figure 3.6).

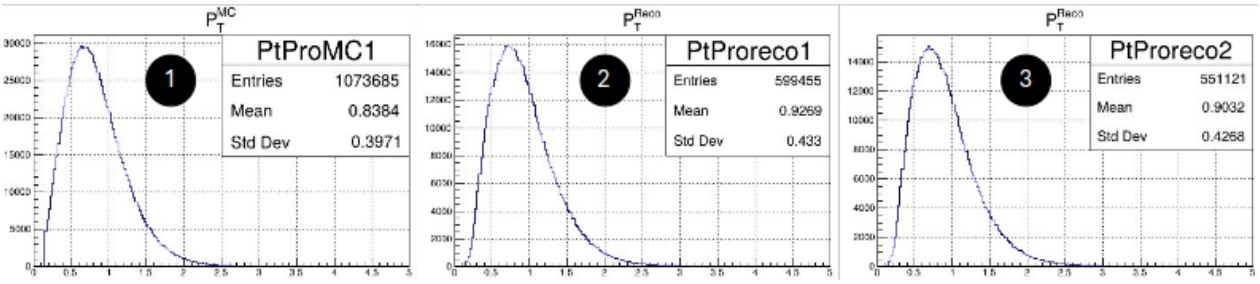

Figure 3.6: *Transverse momentum histograms for the proton, in all three cases: 1- pT histogram for MC tracks using PDG, 2-pT histrogram for reconstructed tracks using dE/dx boundaries, 3-pT histrogram for reconstructed tracks using dE/dx boundaries + PDG code. The change in the number of detected particles is noticeable.*

Then, using another macro [5] we proceeded to divide the histograms obtained, according to the equation (3.2), to obtain the efficiency histograms (figure 3.7), this would indicate how

[5]This macro can be consulted on the page of GitHub [10] in the path: AlejandroSJuan/EnerClass/Efficiency

good or bad the particle reconstruction and identification was, as well as showing in which pT region more particulate contamination may exist.

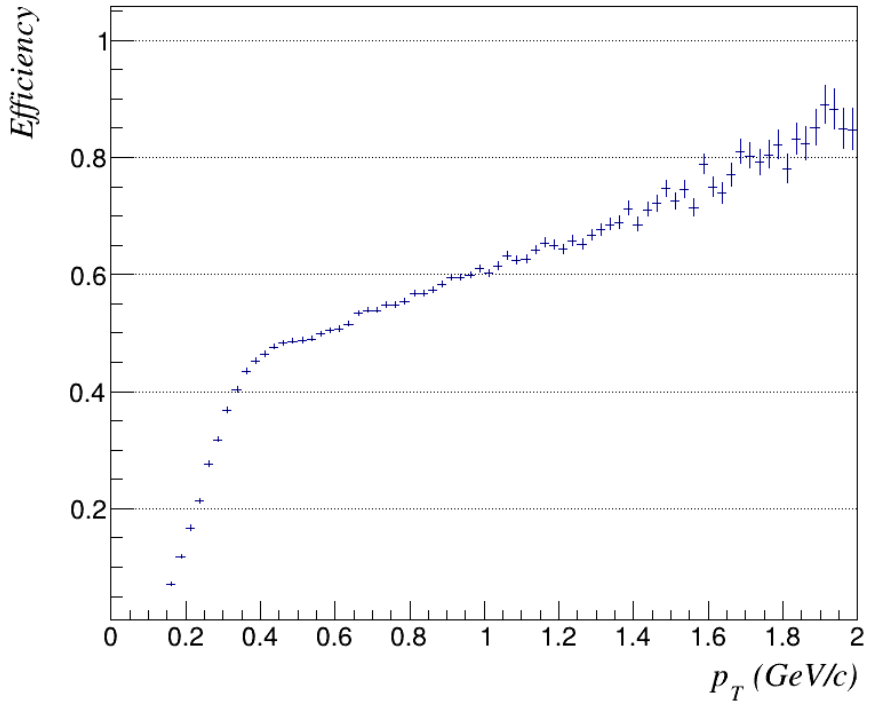

Figure 3.7: *Efficiency histogram for the proton, obtained from dividing the histograms of reconstructed pT between pT monte carlo.*

$$Efficiency = \frac{right\ identified\ tracks}{alltrcks} = \frac{pT\ of\ reconstructed\ tracks}{pT\ of\ Monte\ Carlo\ tracks} \tag{3.2}$$

Chapter 4

Results

1 Adjustment functions for each particle species

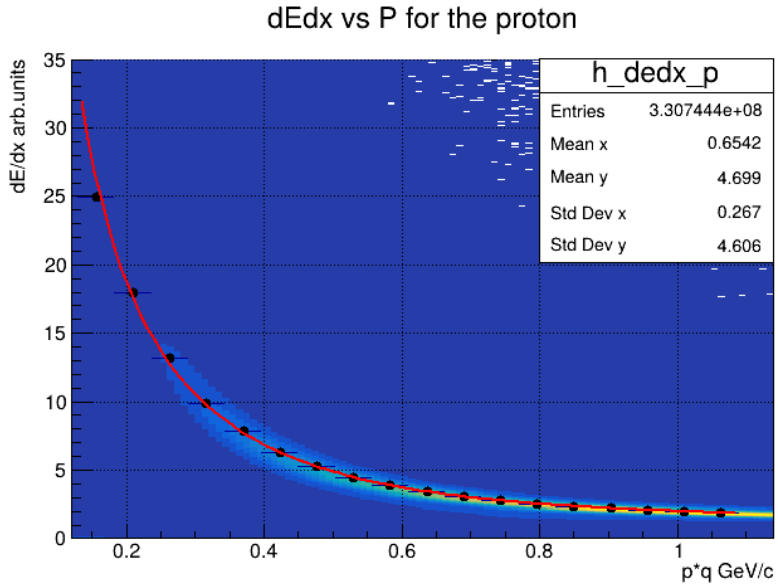

Figure 4.1: *Bethe-Bloch equation adjusted for the proton distribution dE/dx.*

Parameter	P0	P1	P2	P3	P4
Value	-1.24869	0.39063	1.51189	0.822324	2.74567

Table 4.1: *Values of the parameters of the Bethe-Bloch equation for the proton.*

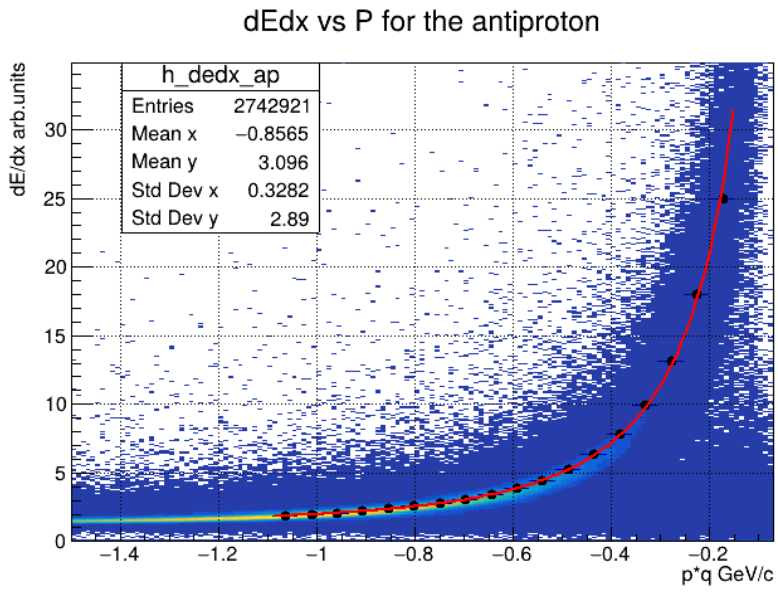

Figure 4.2: *Bethe-Bloch equation adjusted for the anti-proton distribution dE/dx.*

Parameter	P0	P1	P2	P3	P4
Value	1.28243	0.440836	1.52238	0.918907	2.65188

Table 4.2: *Values of the parameters of the Bethe-Bloch equation for the anti-proton.*

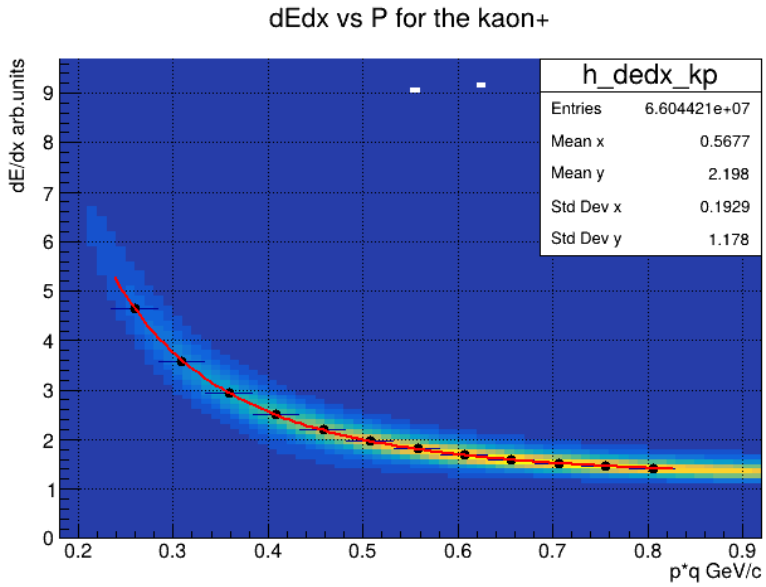

Figure 4.3: *Bethe-Bloch equation adjusted for the kaon distribution dE/dx.*

Parameter	P0	P1	P2	P3	P4
Value	-0.840168	-0.248299	1.14096	0.961078	2.70282

Table 4.3: *Values of the parameters of the Bethe-Bloch equation for the kaon.*

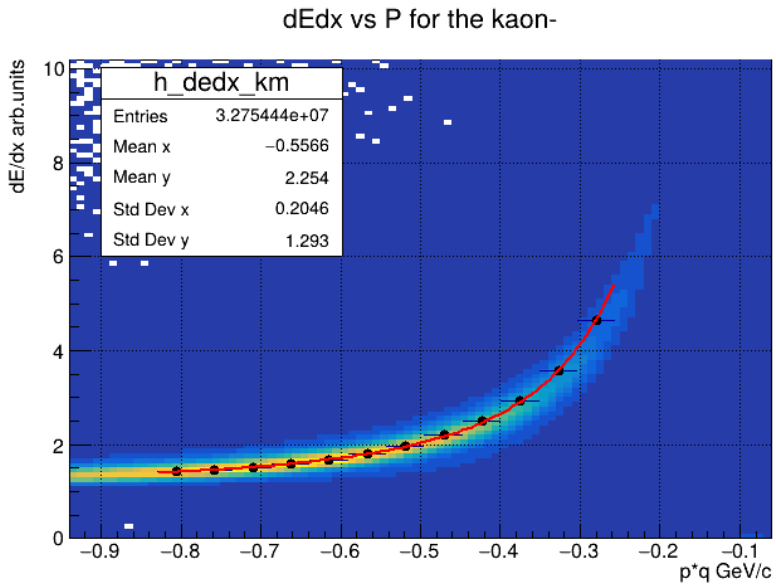

Figure 4.4: *Bethe-Bloch equation adjusted for the anti-kaon distribution dE/dx.*

Parameter	P0	P1	P2	P3	P4
Value	0.752021	-0.103415	1.38771	1.67985	1.95285

Table 4.4: *Values of the parameters of the Bethe-Bloch equation for the anti-kaon.*

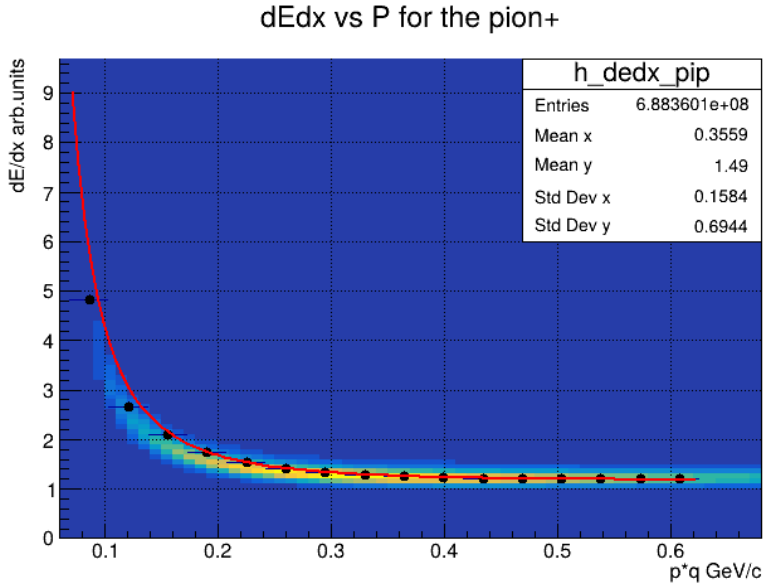

Figure 4.5: *Bethe-Bloch equation adjusted for the pion distribution dE/dx.*

Parameter	P0	P1	P2	P3	P4
Value	-0.25941	-2.71861	-0.163347	3.5057	-0.442799

Table 4.5: *Values of the parameters of the Bethe-Bloch equation for the pion.*

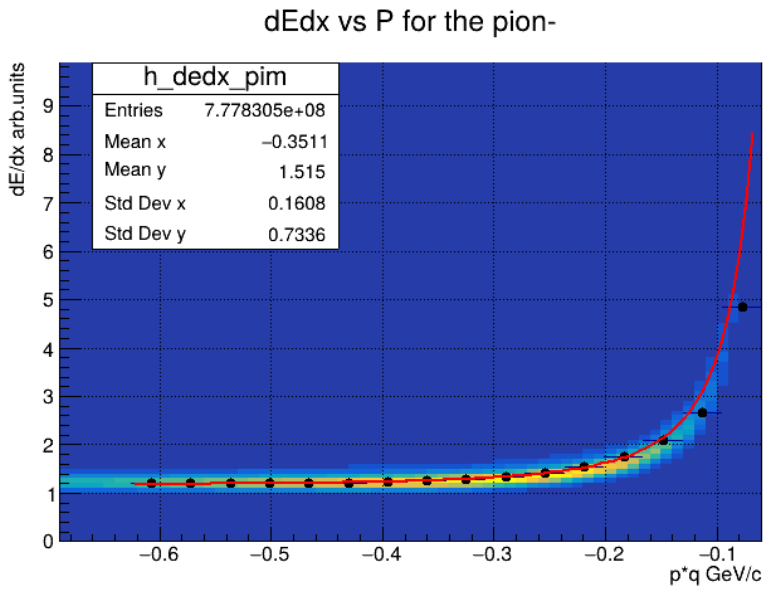

Figure 4.6: *Bethe-Bloch equation adjusted for the anti-pion distribution dE/dx.*

Parameter	P0	P1	P2	P3	P4
Value	0.319817	-2.3113	-0.222699	3.21182	-0.244959

Table 4.6: *Values of the parameters of the Bethe-Bloch equation for the anti-pion.*

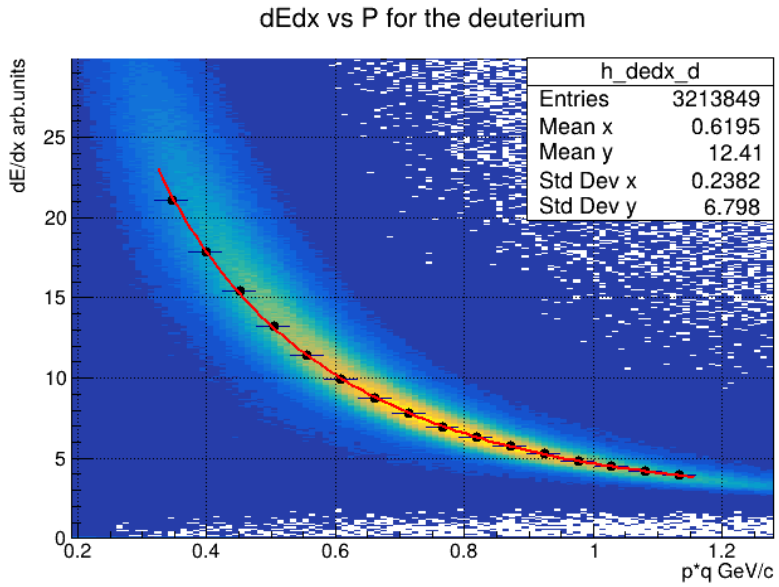

Figure 4.7: *Bethe-Bloch equation adjusted for the deuterium distribution dE/dx.*

Parameter	P0	P1	P2	P3	P4
Value	-2.36254	2.0893	7.6792	0.46067	3.38548

Table 4.7: *Values of the parameters of the Bethe-Bloch equation for the deuteruim.*

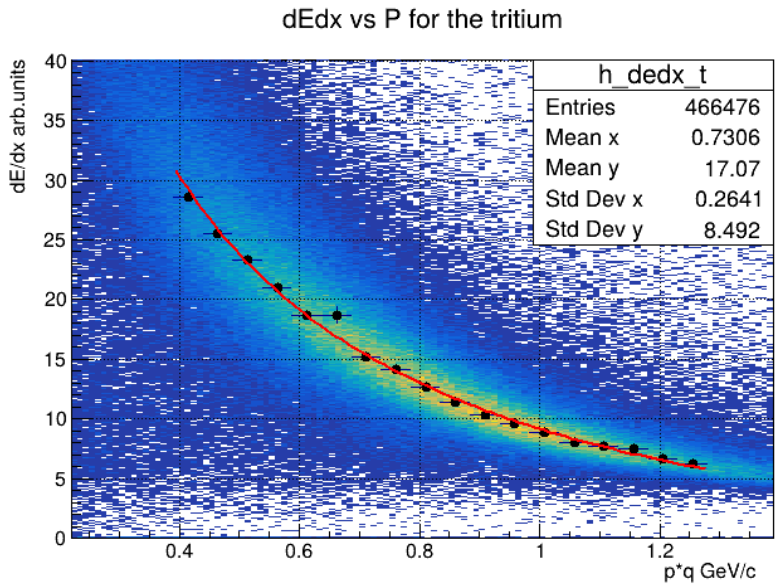

Figure 4.8: *Bethe-Bloch equation adjusted for the tritium distribution dE/dx.*

Parameter	P0	P1	P2	P3	P4
Value	-3.71436	1.89034	1.77948	0.39906	2.64728

Table 4.8: *Values of the parameters of the Bethe-Bloch equation for the tritium.*

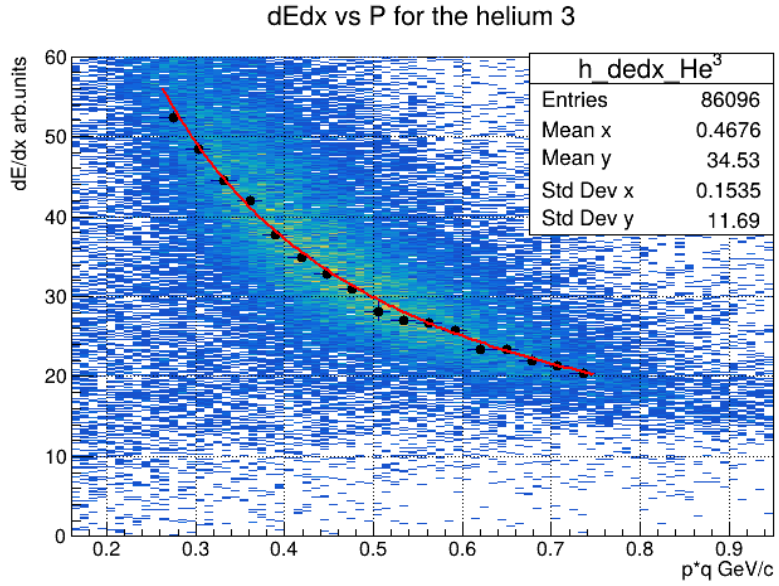

Figure 4.9: *Bethe-Bloch equation adjusted for the He^3 distribution dE/dx.*

Parameter	P0	P1	P2	P3	P4
Value	-27.8842	0.603896	-0.0620607	0.533852	0.385363

Table 4.9: *Values of the parameters of the Bethe-Bloch equation for He^3.*

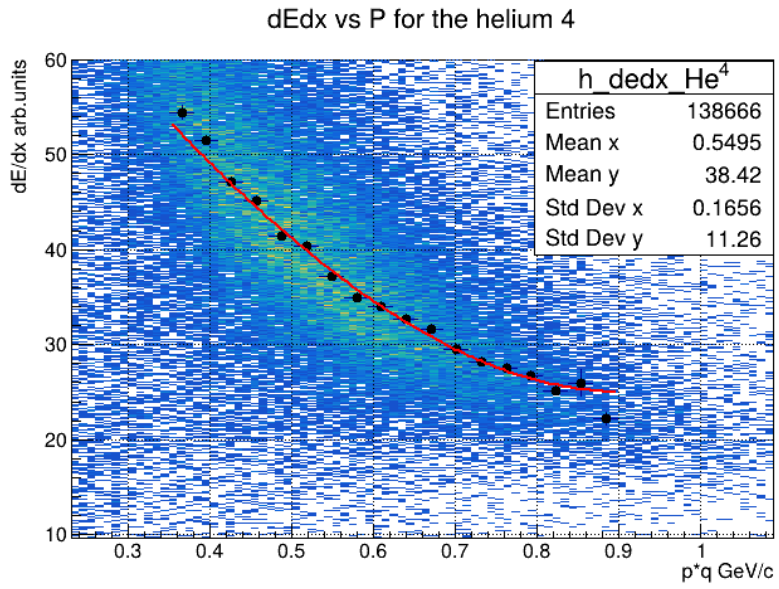

Figure 4.10: *Bethe-Bloch equation adjusted for the He^4 distribution dE/dx.*

Parameter	P0	P1	P2	P3	P4
Value	-100.215	-2.63217	0.00619319	-0.698626	-4.1066

Table 4.10: *Values of the parameters of the Bethe-Bloch equation for He^4.*

It can be observed that for most particles the Bethe-Bloch equation (equation (3.1)) correctly adjusts the energy loss distributions, however, for some cases such as the pion, tritium, He3 and He4; the adjustment function does not exactly pass through all points, which may be due to the fact that when performing projections in dE/dx and obtaining values for mean value and standard deviation, the cuts from the table 3.2had not yet been applied in the energy loss distributions, which prevented us from obtaining more accurate values of the maximum of the Gaussian function (degrees of freedom).

2 Energy loss distributions

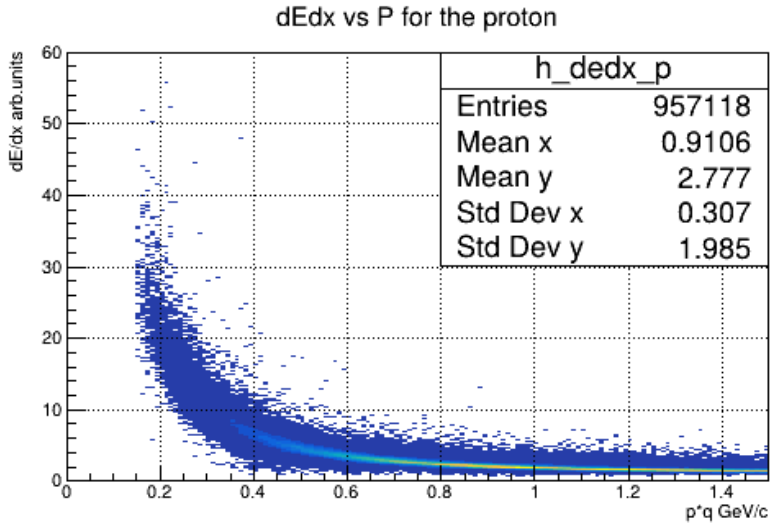

(a) Distribution of dE/dx with PDG code.

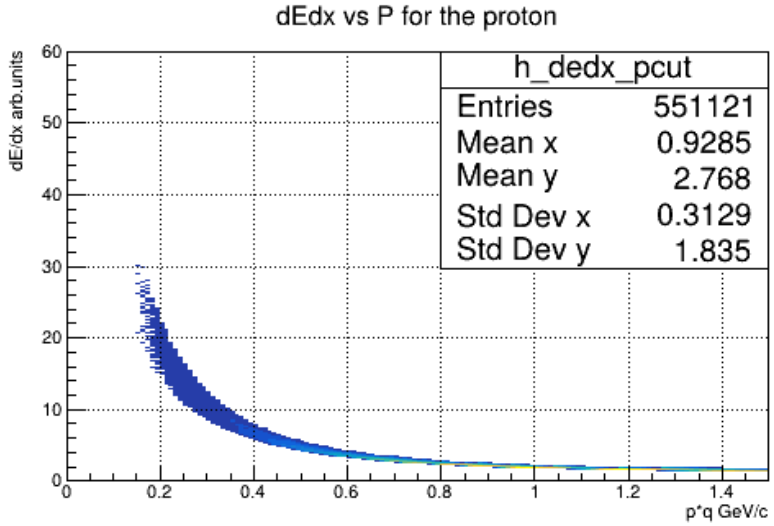

(b) Distribution of dE/dx with limits on the value of dE/dx and PDG code.

Figure 4.11: *Energy loss distributions for primary particles of the proton before and after removing contaminant particles.*

According to the number of entries, it is observed that the percentage of particles after of removed the contaminant particles is approximately 57.5%, This makes sense if we take into account that only the value of a standard deviation σ is taken to delimit the region of highest particle density, which means that the parameters used for limit functions are good, although they can be improved.

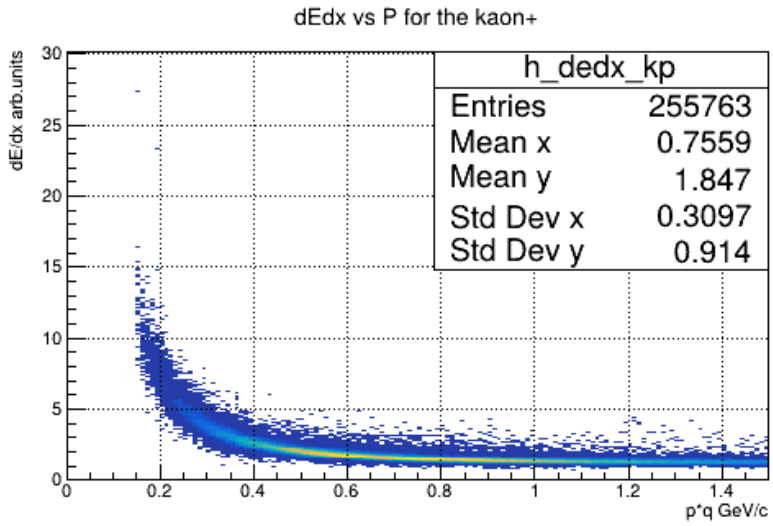

(a) Distribution of dE/dx with PDG code.

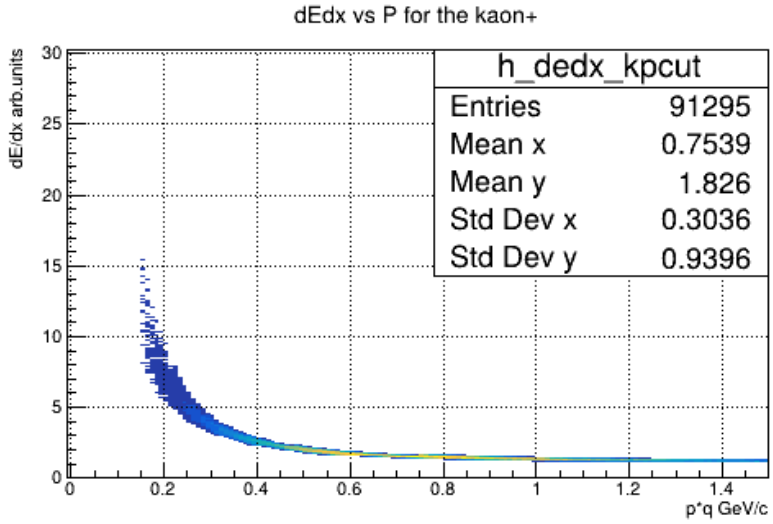

(b) Distribution of dE/dx with limits on the value of dE/dx and PDG code.

Figure 4.12: *Energy loss distributions for primary particles of the kaon before and after removing contaminant particles.*

According to the number of entries, it is observed that the percentage of particles after of removed the contaminant particles is approximately 35.7%, this is not meaningful, because the value for standard deviation chosen was $\pm 1\sigma$, which indicates that we should at least have a value of approximately 68%.

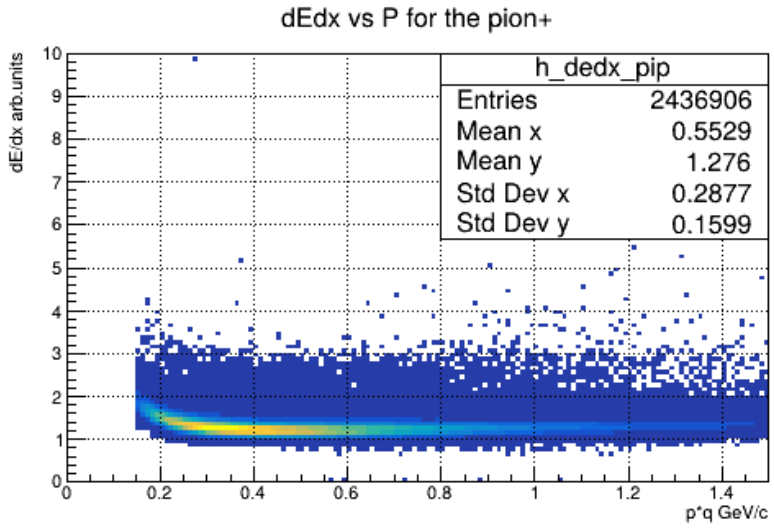

(a) Distribution of dE/dx with PDG code.

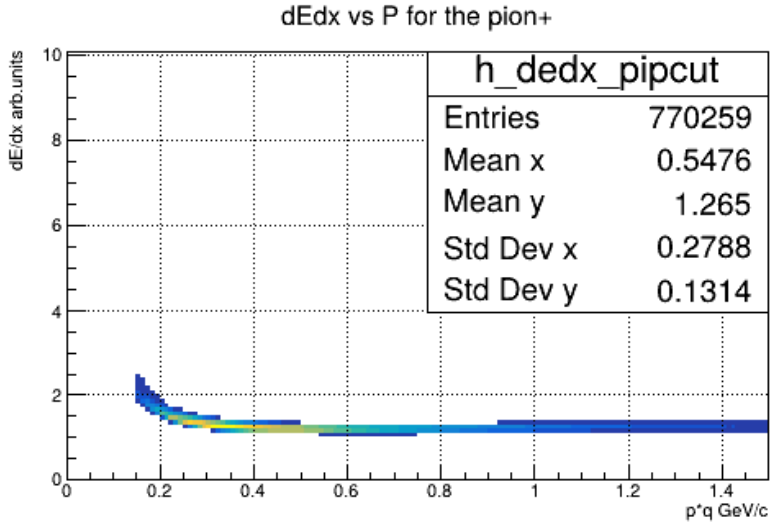

(b) Distribution of dE/dx with limits on the value of dE/dx and PDG code.

Figure 4.13: *Energy loss distributions for primary particles of the pion before and after removing contaminant particles.*

According to the number of entries, it is observed that the percentage of particles after of removed the contaminant particles is approximately 31.6%, this is not meaningful, because the value for standard deviation chosen was $\pm 1\sigma$, which indicates that we should at least have a value of approximately 68%.

3 Efficiency histograms

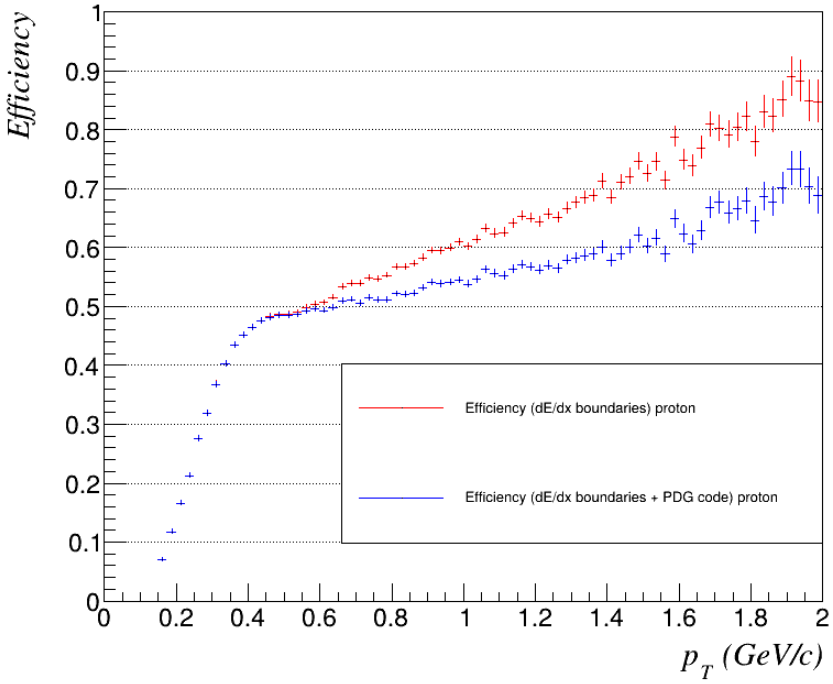

Figure 4.14: *Comparison of the efficiency obtained from protons reconstruction by removing contaminant particles by dE/dx value restriction and PDG code classification.*

As seen in the histogram, the efficiency distribution for primary particles only with dE/dx limits is very similar to the case with PDG code + limits in dE/dx, indicating that the delimitation made with $\pm 1\sigma$ is good, although it could be improved by obtaining more accurate values for σ.

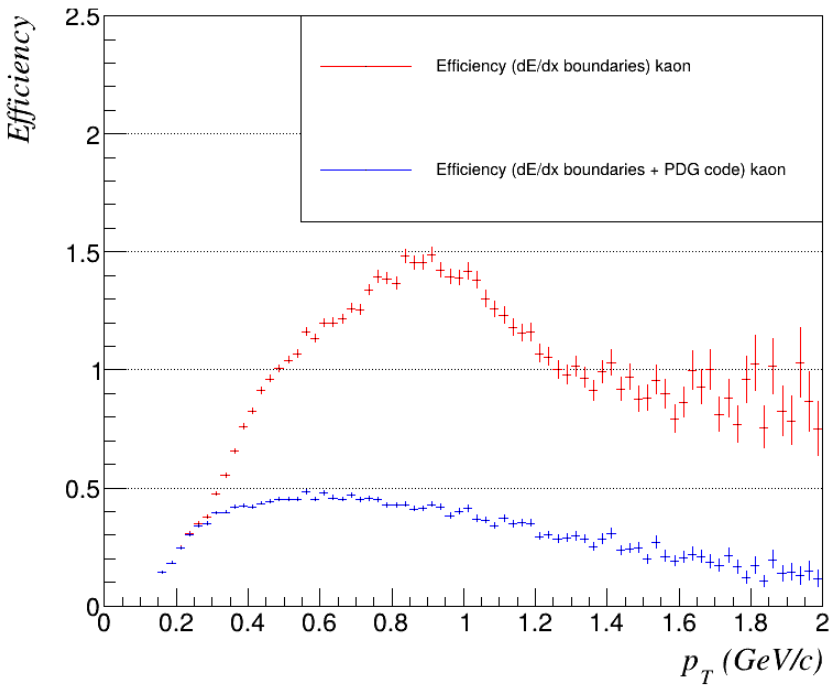

Figure 4.15: *Comparison of the efficiency obtained from kaons reconstruction by removing contaminant particles by dE/dx value restriction and PDG code classification.*

For the case of kaon efficiency distributions, we noticed a clear behavior when taking into account only the pT histogram delimited by the restriction in the value of dE/dx, because unlike the behavior that should be expected (blue dots) there is an increase greater than 1 in a region of 0.6 to 1.2 pT, that is, we will have poor particle identification and increased contamination in this region. The problem may be caused by a bad selection of σ, in addition to not having an accurate value.

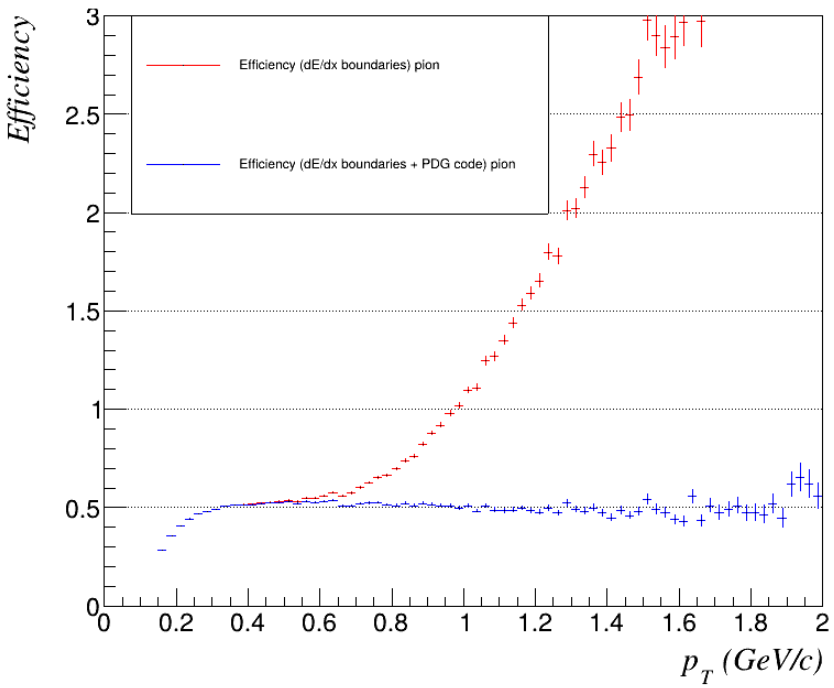

Figure 4.16: *Comparison of the efficiency obtained from pions reconstruction by removing contaminant particles by dE/dx value restriction and PDG code classification*

As for kaons, the efficiency of piones with restriction only on the dE/dx value follows a different trend than expected (blue dots), starting from a pT value greater than 0.6. Again this would indicate that the choice of $\pm 1\sigma$ was not the best, as the number of correctly identified particles is not good, while the amount of contaminating particles increases with the pT value.

Chapter 5

Conclusions

It is known that to achieve a correct identification of a particle species the information in set of each detector or endcaps (TPC + TOF + ECal) is necessary, because it increases the probability of identifying a specific particle by better parametrizing the distributions of dE/dx and m^2.

Although this work showed only the study of the parameterization of energy loss for different particles such as: $P^{\pm}$, $\kappa^{\pm}$, $\pi^{\pm}$, $d^{\pm}$, $t^{\pm}$, $He^{3\pm}$ and $He^{4\pm}$. And specifically what happens to the proton (P^{+}), kaon (κ^{-}) and pion (π^{+}) when obtaining their efficiency histograms without making use of their ideal classification PDG and using only that obtained by parametrizing their energy, Thus, results are not so satisfactory, since the only particle which follows a proper behaviour is the proton, whereas kaon and pion do not. One of the problems is thought to be due to the value obtained from the standard deviation (σ), as mentioned in part of the text this value was obtained after implementing the cuts for the case of the reduced magnetic field, The result is not so accurate, which affects the time of delinking the region of highest particle density.

It is expected to continue this analysis from Mexico in order to clarify what happens not only with these specific particles, but with all the others and also to implement the information provided by each detector for better identification by species of particles.

Chapter 6

Acknowledgments

Express my gratitude to Dr. Ivonne Maldonado for her valuable advice, support and patience in guiding me in the implementation of assigned activities, as well as for her availability for meetings and discussions beyond the established schedules. Also, I thank Dr. Vadim Kolesnikov for his valuable contributions and guidance. In addition, I would like to thank Natalia Komoloyets and Dr. Viktar Kireyeu for their advice and discussions on the activities carried out under the START programme.

Bibliography

[1] Abelev, B. I. et al. (STAR collaboration) (2007). *Measurements of Strange Particle Production in p+p Collisions at $\sqrt{s}$= 200 GeV.* Phys. Rev. C 75, 064901. http://dx.doi.org/10.1103/PhysRevC.75.064901

[2] Abgaryan, V. et al. (MPD Collaboration). (2022). *Status and initial physics performance studies of the MPD experiment at NICA.* Eur. Phys. J. A 58, 140.

[3] Adam, J. et al. (STAR collaboration) (2020). *Bulk properties of the system formed in Au+Au collisions at $\sqrt{S_{NN}}$ =14.5 GeV at the BNL STAR detector.* Phys. Rev. C 101, 024905. https://api.semanticscholar.org/CorpusID:199543556

[4] Adamczyk, L. et al. (STAR Collaboration). *Bulk properties of the medium produced in relativistic heavy-ion collisions from the beam energy scan program.* Phys. Rev. C 96, 044904. http://dx.doi.org/10.1103/PhysRevC.96.044904

[5] CERN. (2009). *Measurement of the Inclusive Jet Cross Section in pp Collisions at $\sqrt{s}$ = 7 TeV Using the ATLAS Detector. CERN Document Server.* Retrieved August 17th, 2024, from https://cds.cern.ch/record/1169055/files/ATL-PHYS-PUB-2009-009.pdf?version=3

[6] Groom,D.E. and Klein, S.R. (2019) *Passage of Particles Through Matter.* Retrieved August 18th, 2024, from https://pdg.lbl.gov/2019/reviews/rpp2018-rev-passage-particles-matter.pdf

[7] Garren, L. (Fermilab),Knowles, I.G. (Edinburgh U.),Navas, S. (U. Granada), Richardson, P. (Durham U.), Sjostrand, T. (Lund U.), and Trippe, T. (LBNL).(2006). *MONTE CARLO PARTICLE NUMBERING SCHEME* Retrieved August 17th, 2024, from https://pdg.lbl.gov/2007/reviews/montecarlorpp.pdf

[8] Iamaldonado. (s.f.). *CoreCoronaTask*. GitHub. Retrieved August 17th, 2024, from https://github.com/iamaldonado/CoreCoronaTask

[9] Iamaldonado. (s.f.). *Macros ANA*. GitHub. Retrieved August 17th, 2024, from https://github.com/iamaldonado/Macros_ANA/blob/main/README.md

[10] Iamaldonado. (s.f.). *START_Summer24*. GitHub. Retrieved August 19 th, 2024, from https://github.com/iamaldonado/START_Summer24/tree/main/AlejandroSJuan

[11] Lechner, A. *Particle Interations with Matter.* CERN Document Server. Retrieved August 17th, 2024, from https://cds.cern.ch/record/2674116/files/660.pdf

[12] Marquez, J. C(2024). *Detector Performance for Reduced Magnetic Field Configuration.* https://start.jinr.ru/index.php

[13] MPDROOT Developers. (s.f.). *MpdPairKK.cxx* . MPDROOT. Retrieved August 18th, 2024, from https://git.jinr.ru/nica/mpdroot/-/blob/v23.03.23/physics/pairKK/MpdPairKK.cxx?ref_type=tags

[14] MPDROOT Developers. (s.f.). *MpdPid.cxx* . MPDROOT. Retrieved August 18th, 2024, from https://git.jinr.ru/nica/mpdroot/-/blob/v23.03.23/core/mpdPid/MpdPid.cxx?ref_type=tags

[15] MPDROOT *Simulation and Analysis Framework for the MPD experiment of the NICA project. (s. f.).* Retrieved August 17th, 2024, from https://mpdroot.jinr.ru/

[16] Multi purpose detector: the Mega-Science Project «NICA». (2024). Retrieved August 17th, 2024, from https://mpd.jinr.ru/

[17] Mudrokh .A (on behalf of the MPD team) (2018). *Particle identification (PID) and prospects for the study of event-by-event fluctuations at MPD* Veksler and Baldin Laboratory of High Energy Physics, JINR, Russia. https://indico.jinr.ru/event/436/contributions/4008/attachments/2986/3843/PID_and_prospects_for_EbEfluct_Mudrokh.pdf

[18] Mudrokh .A (on behalf of the MPD team) . *Particle Identification (PID) as a tool for the study of event-by-event fluctuations atMPD.* Veksler and Baldin Laboratory of High Energy Physics, JINR, Russia. https://indico.cern.ch/event/656452/contributions/2919504/attachments/1648156/2634899/PID_as_a_tool_for_EvE_study_MPD.pdf

[19] NICA - Nuclotron-based Ion Collider FAcility. (s.f.). Retrieved July 14th, 2024, from https://nica.jinr.ru/complex.php

[20] Raghunath Sahoo. (2013). *Relativistic Kinematics.* E-print: 1604.02651 [nucl-ex] https://arxiv.org/pdf/1604.02651.pdf

[21] San Juan .A (2023) . *MPD detector performance study at the NICA collider.* https://interest.jinr.ru/